

## RESEARCH CONCERNING THE SUPERFICIAL LAYER AT CLASSIC AND ULTRASONIC AIDED ELECTRICAL DISCHARGE MACHINING

<sup>1</sup>DUCA M. Anca-Valentina, <sup>1</sup>RĂSCOL S. Viorica and <sup>2</sup>GHICULESCU Liviu Daniel

<sup>1</sup>Faculty of Industrial Engineering and Robotics, Study program: Machine Building Technology,  
Year of study: IV, e-mail: [ancavalentina2202@gmail.com](mailto:ancavalentina2202@gmail.com)

<sup>2</sup>Faculty of Industrial Engineering and Robotics, Manufacturing Engineering Department

*ABSTRACT: The paper deals with a comparative study of superficial layer of CoCr alloys obtained at classic and ultrasonic (US) aided electrical discharge machining (EDM). The machined materials characteristics, the equipment used at laboratory experiments, the working values and the most relevant images of superficial layer provided by scanning electron microscope are presented. Comparative numerical simulation of discharges in case of EDM and EDM+US and their effect on the superficial layer were validated by experimental data.*

*KEYWORDS: superficial layer, electroerosion, ultrasound, numerical simulation.*

### 1. Introduction

Considering the challenges brought by advanced technologies, electrical discharge machining (EDM) is one of the best alternatives for processing an increasing number of conductive materials with high hardness, non-corrosive and wear-resistant properties [1, 2]. EDM with electrode vibration normal to the processed surface at ultrasonic frequency is characterized by a significant improvement in the main EDM parameters - increased productivity, reduced relative volumetric wear, roughness of the processed surface and the melted and resolidified surface layer [3].

### 2. The current stage regarding the superficial layer resulting from EDM

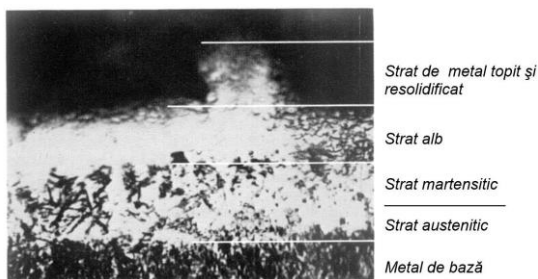


Fig. 1 Surface layer structure, EDM [4]

Surface quality involves both roughness and the structure of the surface layer affected by EDM, namely the thermal influence area. The structure of the surface layer is represented by the austenitic layer, the martensitic layer, the white layer, and the melted and resolidified metal layer - Fig. 1 [4].

Following an electrical discharge, a crater is formed. The material remaining in the craters resolidifies and is called the white layer because it has this color when viewed under a microscope. It is not chemically attacked by usual agents (e.g. nital).

[5]. It exhibits numerous micro-cracks as a result of exceeding the rupture strength caused by the thermal shock generated by discharges. Further down, a high surface hardness martensitic layer is encountered (about 1000 HV at a depth of 25  $\mu\text{m}$ ) followed by an austenitic layer, typical hardening constituents resulting from the rapid heating and cooling process of EDM. Ultrasonic assistance (US) in EDM finishing (EDM+US) significantly reduces the white layer and hence internal stresses (by about 50%), increasing fatigue resistance (2...6 times) [4].

### 3. Characteristics of processed CoCr alloys and equipment used

In general, Co-Cr alloys can be described as alloys with high wear and temperature resistance, non-magnetic, with excellent biocompatibility, corrosion resistance, and a high elastic modulus, which also ensures appropriate rigidity [6]. The chemical composition of the two alloys chosen for the study, named System NE and System SOFT, is presented in Table 1, and the mechanical characteristics that influence the layer of solid material removed by US are shown in Table 2.

**Table 1 Chemical composition of CoCr alloys [7]**

Alloy	Cr [%]	Mo [%]	W [%]	Nb [%]	Si [%]	Mn [%]	Fe [%]	Co [%]
P1, SYSTEM NE	21,0	6,5	6,4	-	0,8	0,65	<0,1	64,4
P2, SYSTEM SOFT	29,5	5,7	-	-	0,95	0,55	0,75	61,8

**Table 2. Mechanical characteristics of CoCr alloys [7]**

Alloy	Ultimate tensile strength [MPa]	Young modulus [GPa]	Yield strength [MPa]	Break elongation [%]	Rigidity [HV]
P1, SYSTEM NE	850	155	580	3	460
P2, SYSTEM SOFT	447	160	450	15	310

Figure 1 shows the working head of the EDM ELER 01 machine, located in the laboratory of the FIIR faculty, TCM department, UPB, on which an ultrasonic chain was mounted, with a copper disc electrode-tool at the end. The cylindrical-shaped samples of the two alloys were machined at one end using conventional EDM and at the other end using EDM in an ultrasonic field, in order to observe and compare the resulting surface layer obtained using the two methods - see Figure 2.

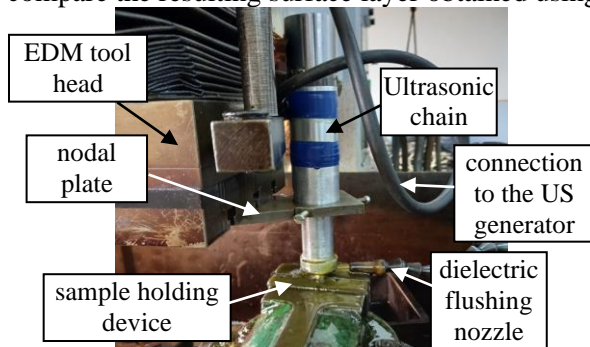


Fig. 2. The tool head of the ELER 01 machine and the US chain mounted on it

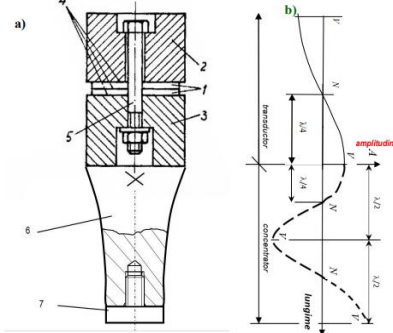


Fig. 3. Ultrasonic chain and standing waves formed within it [3]

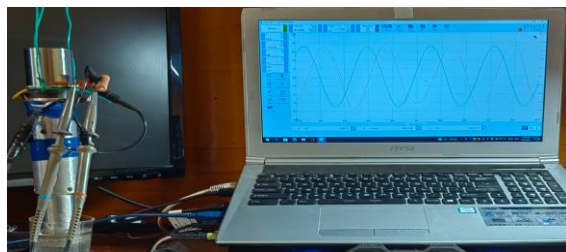


Fig. 4. Determination of the natural frequency ( $f_0=19.21$  kHz) of the ultrasonic chain and adjustment of the generator at resonance

The US chain, fig. 3.a, presents a transducer with piezoceramic plates 1 that change their dimensions, connected in a variable electric field given by a US generator, transmitting vibrations, standing waves, fig. 3.b along the US chain. The transducer also includes the reflecting bushing (2), Cu blades (4) for connection to the US generator, the radiating bushing (3) and the screw (5) that assembles the pre-stressed transducer components with 8-10 tf. The amplification of US oscillations is achieved through the horn 6, at the end of which the tool 7 is located (positioned in the antinode). The natural frequency,  $f_0=19.21$  kHz, of the US chain was determined and the US generator was adjusted to the same frequency to obtain resonance - fig. 4.

#### 4. Experimental data regarding the obtained surface layer

The distribution of chemical elements in the surface layer structure of the processed alloys is presented in fig. 5, System NE and fig. 6, System Soft. This was obtained with the EDAX system, generating X-rays from samples processed by scanning with the electron beam of the SEM QUANTA INSPECT F50 - UPB microscope, with a resolution of 1 nm. A reduction in the depth of the C-enriched layer was observed due to the US effect, by collecting a larger amount of melted material by breaking the gas bubble formed around the plasma channel of the discharge at the end of a US oscillation.

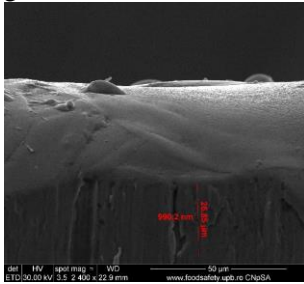
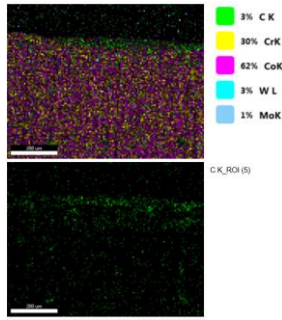
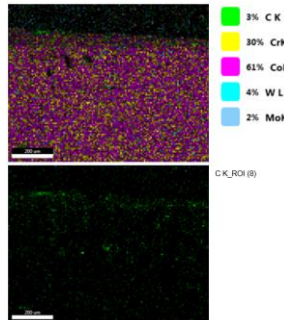


Fig. 5. Microcrack for EDM+US System NE

Thus, for the System NE alloy, the thickness of the layer with significant C content (green color) is approximately 200 μm for classic EDM and approximately 100 μm for EDM+US - see the white reference point, Fig. 6; it was machined with a current  $I=12$  A and pulse time  $t_i=95$  μs, while the power of the US generator was  $P_{us}=80$  W. In the case of the System Soft alloy, the thickness of the layer with high C content is 500 μm for classic EDM and approximately 50 μm for EDM+US - see the white reference point, Fig. 7; it was machined with  $I=12$  A and  $t_i=24$  μs,  $P_{us}=80$  W. This layer with microcracks, produced by the thermal shock of the EDM discharge (Fig. 5) called the white layer, is greatly reduced in the case of EDM+US.

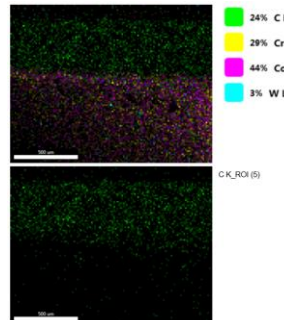


a. System NE - EDM

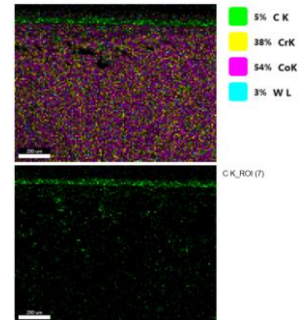


b. System NE - EDM+US

Fig. 6. Repartition of the chemical elements in the composition of System NE in the structure of the superficial layer.

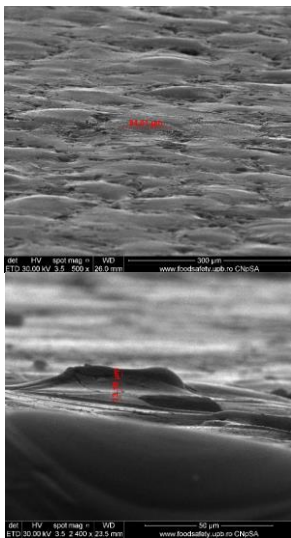


a. System Soft - EDM

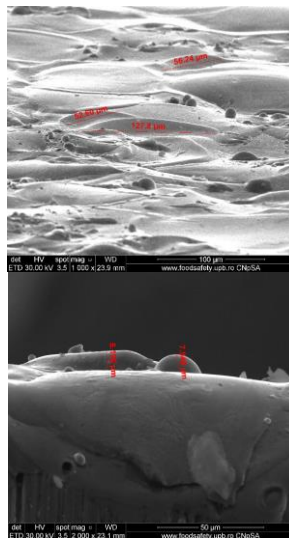


b. System Soft - EDM+US

Fig. 7. Repartition of the chemical elements in the composition of System SOFT in the structure of the superficial layer.

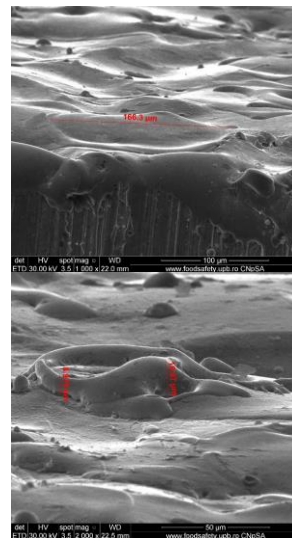


a. System NE - EDM

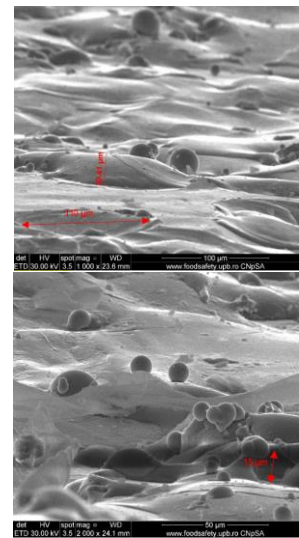


b. System NE - EDM+US

Fig. 7. Microgeometry of the machined surface at System NE; dimensions of craters (top) and protrusions (bottom)



a. System Soft - EDM



b. System Soft - EDM+US

Fig. 8. Microgeometry of the machined surface at System SOFT; dimensions of craters (top) and protrusions (bottom)

The images of the microgeometry of the machined surface obtained with the same SEM microscope at the same processing parameters as before are presented comparatively in Fig. 7, 8. It can be observed that for both materials, at EDM+US compared to EDM, the dimensions of the craters are smaller, and the height of the protrusions is higher for System Soft (lower mechanical resistance to US action) compared to System NE.

### 5. Numeric simulation of the classic and ultrasonic electrical discharge machining

To study the material removal mechanisms in EDM+US, Comsol Multiphysics was used in 2D axisymmetric space, with the Heat Transfer in Solids module for the EDM component and the Solid Mechanics module for the US component, both time-dependent. The following steps were taken:

(1) Parameterization of the thermal and mechanical models for both materials studied, fig. 9, 10;

Name	Expression	Description	Name	Expression	Description
hp	15[mm]	inaltime piesa de proba	TiCoCr	3000	Temperatura de fierbere [C]
rp	4[mm]	raza piesei de proba	TmCoCr	1330	Temperatura de topire [C]
l	12	treapta de curent	rcp	$1e-6 \cdot 2.161 \cdot 10^{0.43} \cdot (t_i \cdot 1e6)^{0.44}$	raza canal plasma dependenta de timp
tif	95e-6	timp de impuls final	ti	0	timp impuls baleiat
acr	47e-6	raza crater initial	a	1e-6	raza initiala canal plasma
bcr	49[μa]	adancime crater initial	hus	1e-6	timp solicitare US
rms	0.8e-6	raza material resolidificat	pus	120[MPa]	presiune ultrasonica
rbg	0.1[mm]	raza bula gaz	sigmar	850[MPa]	rezistenta la rupere statica NE
Ra	5.5e-6	Ra suprafata prelucrata	taud	211.2	rezistenta la oboseala forfecare NE

Fig. 9. Model parameters System NE

Name	Expression	Value	Description	Name	Expression	Description
hp	15[mm]	0.015 m	inaltime piesa de proba	TiCoCr	3000	Temperatura de fierbere [C]
rp	4[mm]	0.004 m	raza piesei de proba	TmCoCr	1330	Temperatura de topire [C]
l	12	12	treapta de curent	rcp	$1e-6 \cdot 17 \cdot 10^{0.43} \cdot (t_i \cdot 1e6)^{0.44}$	raza canal plasma dependenta de timp
tif	24e-6	2.4E-5	timp de impuls final	ti	0	timp impuls baleiat
acr	83e-6	8.3E-5	raza crater initial	a	1e-6	raza initiala canal plasma
bcr	49[μa]	2.2E-5	adancime crater initial	tus	1e-6	timp solicitare US
Ra	5.5e-6	5.5E-6	Ra suprafata prelucrata	pus	120[MPa]	presiune ultrasonica
rms	0.8e-6	8.0E-7	raza material resolidificat	sigmar	447[MPa]	rezistenta la rupere statica SOFT
rbg	0.3[mm]	3.0E-4 m	raza bula gaz	taud	133.8	rezistenta la oboseala SOFT

Fig. 10. Model parameters System SOFT

(2) The geometry (EDM), time-dependent plasma channel radius - fig. 11); (3) Meshing - fig. 12;

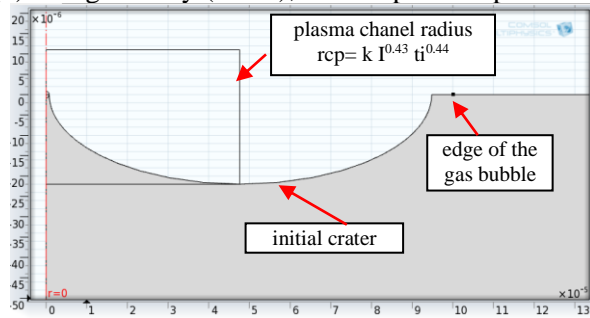


Fig. 11. Geometry of the models in the area of interest

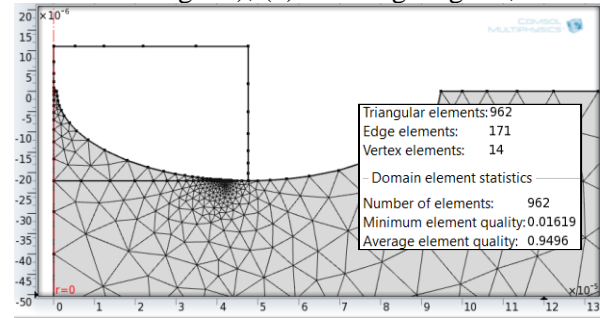


Fig. 12. Discretization, statistics and their quality

(4) Introducing material characteristics for System NE alloy - fig. 13 and System Soft - fig. 14;

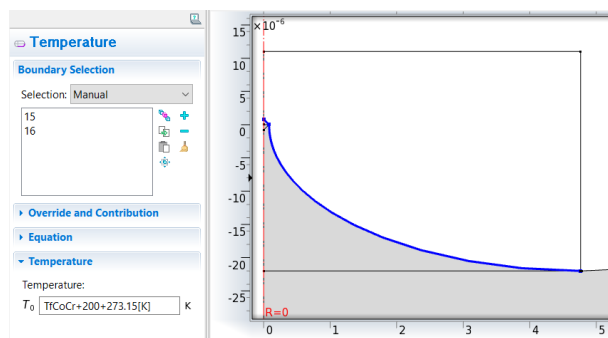
Property	Name	Value	Unit
✓ Thermal conductivity	k	14.5	W/(m*K)
✓ Density	rho	8400	kg/m^3
✓ Heat capacity at constant pressure	Cp	390	J/(kg*K)
✓ Young's modulus	E	155[GPa]	Pa
✓ Poisson's ratio	nu	0.3	1

Fig. 13. Material characteristics, System NE

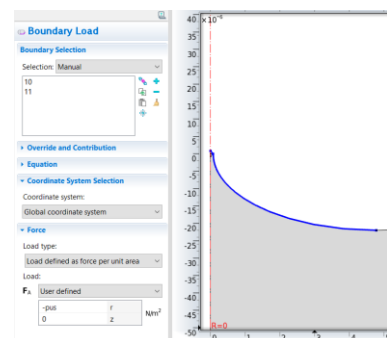
Property	Name	Value	Unit
✓ Thermal conductivity	k	13.08	W/(m*K)
✓ Density	rho	8250	kg/m^3
✓ Heat capacity at constant pressure	Cp	390	J/(kg*K)
✓ Young's modulus	E	160[GPa]	Pa
✓ Poisson's ratio	nu	0.3	1

Fig. 14. Material characteristics, System SOFT

(5) Introducing boundary conditions for the thermal module - fig. 15 and the mechanical module - fig. 16

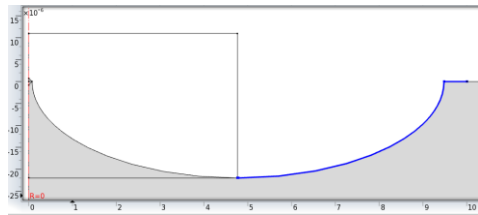


a) temperature at the EDM spot, time-dependent radius

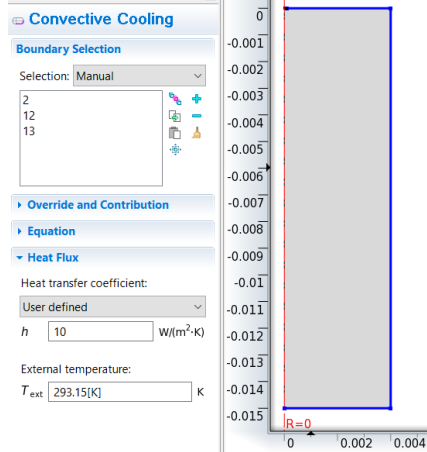


a) cyclic load of the ultrasonic pressure

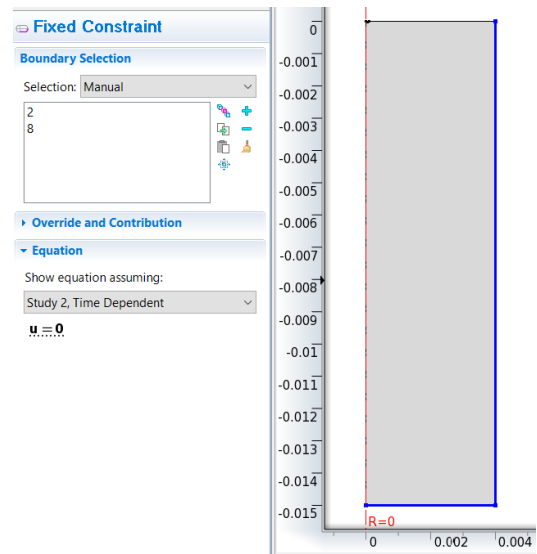




b) thermal insulation produced by the gas bubble



c) convective cooling - workpiece in contact with dielectric  
Fig. 15. Boundary conditions - thermal module - EDM



b) fixed surfaces of the workpiece - holding method  
Fig. 16. Boundary conditions - mechanical module - US

## 6. Numerical simulation results

A single discharge was simulated with the thermal module under classical EDM conditions, obtaining the temperature distributions shown in figures 17 and 18. These show the position of the boiling isotherm at the end of the pulse time, which delimits the volume of material removed, according to the overheating model [8]. Values for radius (red arrow) and depth (blue arrow) are validated by real data.

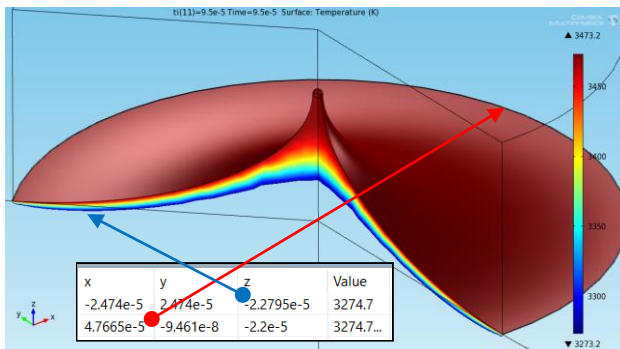


Fig. 17. Boiling isotherm at  $t_i=95 \mu\text{s}$ , System NE

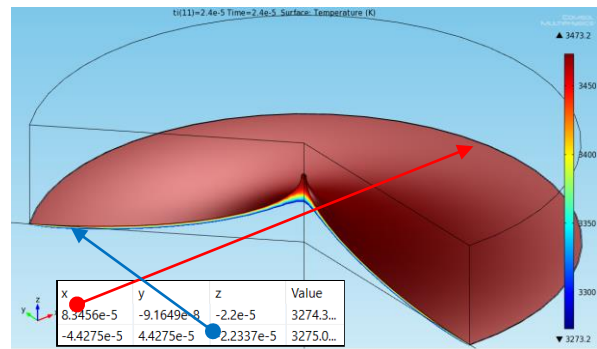


Fig. 18. Boiling isotherm at  $t_i=24 \mu\text{s}$ , System SOFT

Running the thermal module under EDM+US conditions shows the position of the melting isotherm - fig. 19, 20. The implosion of the gas bubble formed around the plasma channel of the discharge at the end of a US oscillation period allows the dielectric liquid to access the EDM spot area, removing the material delimited by the melting isotherm [8]. Thus, the thickness of the white layer, which comes from the C-enriched melted material of the discharge, becomes much smaller under EDM+US conditions. The probability that the US waves will remove all the melted material is around 30% [8]. For this to happen, the end of the US period ( $T_{us}$ ) must overlap with the duration of the discharge. For the remaining craters where removal occurs through boiling (the discharge does not overlap the end of  $T_{us}$ ), the mechanical material removal caused by the shock waves of the US cavitation, which generate pressures of the order of 100 MPa, acts - fig. 21, 22.

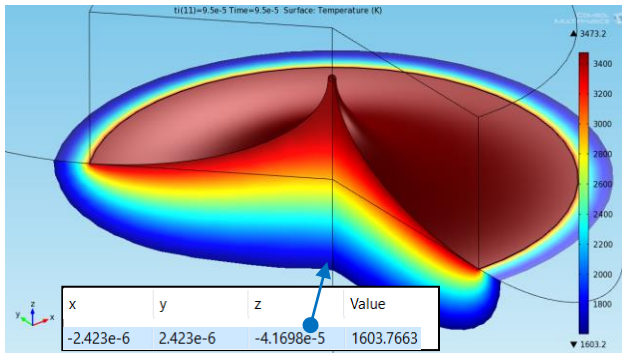


Fig. 19. Melting isotherm at  $t_i=95 \mu s$ , System NE  
Time=1e-6 Surface: von Mises stress (MPa)

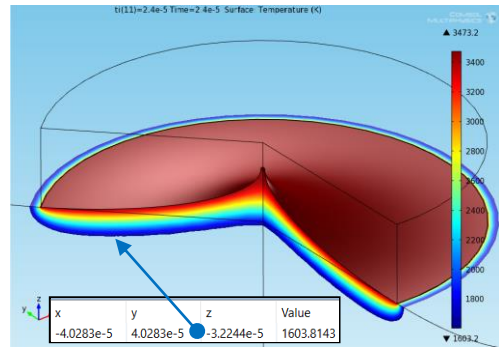


Fig. 20. Melting isotherm at  $t_i=24 \mu s$ , System SOFT  
Time=1e-6 Surface: von Mises stress (MPa)

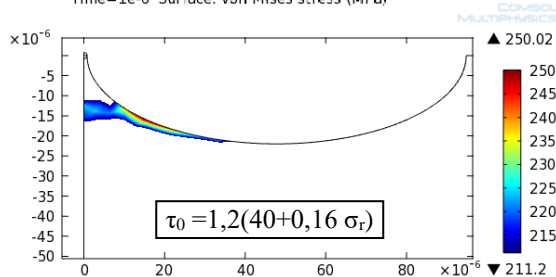


Fig. 21. US removal at System NE,  $\tau_0 = 211.2 \text{ MPa}$

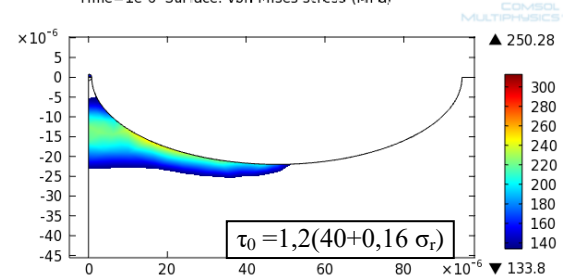


Fig. 22. US removal at System SOFT,  $\tau_0 = 133.8 \text{ MPa}$

## 7. Conclusions

A numerical simulation of the thermal and mechanical material removal during EDM+US was performed, compared to classical EDM, and validated by experimental data. The ability of US to reduce the superficial white layer containing microcracks is highlighted. The reduction is greater in the case of CoCr alloy System SOFT, compared to System NE, due to lower mechanical resistance to cyclic shear stress produced by the ultrasonic cavitation at the end of  $T_{us}$  period. Future research will focus on minimizing the white layer through EDM+US and determining the processing regime, with the key parameter being the ultrasonic pressure ( $P_{us}$ ), which is adjusted by the power from the US generator.

## 8. Bibliography

- [1]. Abu Zeid, O.A. (1997). On the effect of electro-discharge machining parameters on the fatigue life of AISI D6 tool steel. J. Mater. Process. Technol., vol. 68, p. 27-32
- [2]. Merdan, M.A.E.R., Arnell, R.D. (1991). The surface integrity of a die steel after electro-discharge machining, 2. residual stress distribution. Surf. Eng., vol. 7, p. 154-158.
- [3]. Ghiculescu, D. (2021), "Ultrasonic machining", Course in Romanian, Production Engineering Dept., University Politehnica from Bucharest, Romania.
- [4]. Ghiculescu, D. (2021), „The main technological parameters at EDM”, Course in Romanian, Production Engineering Dept., University Politehnica from Bucharest, Romania.
- [5]. Shabgard, M., Seyedzavvar, M., Oliaei, S. N. B. (2014). „Influence of input parameters on characteristics of EDM process”, University of Tabriz, Tabriz, Iran
- [6]. Comăneanu, R. M. (2020), “Studies on biomaterials properties, simulations, and applications in dental implantology and prosthesis”, In Romanian, Department of Dental Medicine, University “Titu Maiorescu” from Bucharest, Romania.
- [7] \*\*\* CoCr Alloys for stomatology, Available at <https://www.dentex.ro/aliaj-co-cr-system-soft-1g>, accessed at: 30.04.2023
- [8]. Ghiculescu, D., Ultrasonically Aided Electrical Discharge Machining, in EDM, Types, Technologies and Applications, Nova Publishers, New York, USA, 2015.